# Humic acid protein complexation

W.F. Tan [a,1], L.K. Koopal [a,*], L.P. Weng [b], W.H. van Riemsdijk [b], W. Norde [a,c]

[a] Laboratory of Physical Chemistry and Colloid Science, Wageningen University, Dreijenplein 6, 6703 HB Wageningen, The Netherlands
[b] Department Soil Quality, Wageningen University, Droevendaalsesteeg 4, 6708 PB Wageningen, The Netherlands
[c] Department Biomedical Engineering, University Medical Center Groningen, A.Densinglaan 1, 9713 AV Groningen, The Netherlands

## Abstract

Interactions of purified Aldrich humic acid (PAHA) with lysozyme (LSZ) are investigated. In solution LSZ is moderately positively and PAHA negatively charged at the investigated pH values. The proton binding of PAHA and of LSZ is determined by potentiometric proton titrations at various KCl concentrations. It is also measured for two mixtures of PAHA–LSZ and compared with theoretically calculated proton binding assuming no mutual interaction. The charge adaptation due to PAHA–LSZ interaction is relatively small and only significant at low and high pH. Next to the proton binding, the mass ratio PAHA/LSZ at the iso-electric point (IEP) of the complex at given solution conditions is measured together with the pH using the Mütek particle charge detector. From the pH changes the charge adaptation due to the interaction can be found. Also these measurements show that the net charge adaptation is weak for PAHA–LSZ complexes at their IEP. PAHA/LSZ mass ratios in the complexes at the IEP are measured at pH 5 and 7. At pH 5 and 50 mmol/L KCl the charge of the complex is compensated for 30–40% by $K^+$; at pH 7, where LSZ has a rather low positive charge, this is 45–55%. At pH 5 and 5 mmol/L KCl the PAHA/LSZ mass ratio at the IEP of the complex depends on the order of addition. When LSZ is added to PAHA about 25% $K^+$ is included in the complex, but no $K^+$ is incorporated when PAHA is added to LSZ. The flocculation behavior of the complexes is also different. After LSZ addition to PAHA slow precipitation occurs (6–24 h) in the IEP, but after addition of PAHA to LSZ no precipitation can be seen after 12 h. Clearly, PAHA/LSZ complexation and the colloidal stability of PAHA–LSZ aggregates depend on the order of addition. Some implications of the observed behavior are discussed.

## 1. INTRODUCTION

As major components of natural organic matter, humic and fulvic acids are involved in many chemical and physical interactions in soil and aqueous systems (Buffle, 1988; Bolto, 1995). Humic substances (HS) are composed of amorphous, chemically complex and internally structured molecules or molecular aggregates (Avena and Wilkinson, 2002; Sutton and Sposito, 2005) with a polyelectrolyte nature that can be classified as soft-colloidal matter (Duval et al., 2005). For the pH conditions in most natural waters HS are negatively charged and the pH affects both the charge density and the hydrodynamic radius of the humic particles (Avena et al., 1999a). Due attention has been paid to the interactions of HS with protons and heavy metal ions (Tipping, 2002; Milne et al., 2003; Koopal et al., 2005; Merdy et al., 2006). Also complexation of HS with oppositely charged polyelectrolytes (Glaser and Edzwald, 1979; Rebhun et al., 1998; Bolto et al., 1999; Kam and Gregory, 1999; Kam and Gregory, 2001; Kvinnesland and Ødegaard, 2004; Hankins et al., 2006) and surfactants (Traina et al., 1996; Adou et al., 2001; Koopal et al., 2004; Ishiguro et al., 2007) has been investigated. The attention paid to the interaction between HS and oppositely charged polyelectrolytes has largely been directed to the removal of HS from aqueous solutions by complexation and aggregation.

* Corresponding author. Fax: +31 317 483777.
  E-mail address: luuk.koopal@wur.nl (L.K. Koopal).
[1] Permanent address: College of Resources and Environment, Huazhong Agricultural University, Wuhan 430070, PR China.

A special class of polyelectrolytes that also may interact with HS are proteins. Yet, little or no literature is available on HS–protein interaction. Binding of proteins to other polyelectrolytes has been investigated because of its importance in technological applications. Reviews of this work can be found in literature (Xia and Dubin, 1994; Kokufuta, 1994; Schmitt et al., 1998; Tribet, 1999; Carlsson et al., 2001; Doublier et al., 2002; Cooper et al., 2005; Bohidar et al., 2005; Gummel et al., 2006). In view of the attention paid to polyelectrolyte–protein interaction, it is somewhat surprising that the binding of HS to proteins has been neglected. This binding can be especially relevant in relation to soil quality. Recent research (Hayes and Edward Clapp, 2001; Nichols and Wright, 2005; Schindler et al., 2007) has indicated that, for instance, the glycoprotein glomaline can be important for soil structure and soil extraction. Also relevant is the role of pathogenic proteins such as insecticidal proteic toxins, pharmaceutical proteins (produced in transgenic plants) and infectious (prion) proteins involved in transmissible spongiform encephalopathies (causing diseases as BSE and Creutzfeldt–Jakob) that may be present in ground and surface waters. HS–protein interaction may lead to modification of the protein structure and, consequently, to a change in its biological activity. The extent to which this occurs depends on the specific conditions (Brouwer et al., 1990; Wen and Dubin, 1997; Xia et al., 1997). Furthermore, binding to other substances makes proteins less susceptible to microbial degradation and this can be environmentally hazardous.

In this paper HS–protein interaction is studied by considering the interaction of purified Aldrich HA (PAHA) with the protein lysozyme (LSZ). PAHA is often used in model studies because it is easily available and studies of various humic acids including Aldrich have shown that the trends in ion and surfactant binding to PAHA are similar to that of other humic acids (Milne et al., 2003; Ishiguro et al., 2007). LSZ is used in model studies because its structure is well known; it has a nearly spherical shape and a good structural stability (Blake et al., 1965; Horsley et al., 1987; Ramanadham et al., 1990; Coffman et al., 1997). LSZ has weak acidic and basic groups and in the natural pH range it has a net positive charge (Haynes et al., 1994; Biesheuvel et al., 2005). A proper investigation of HA–LSZ binding and flocculation will be a very first step towards understanding HS–protein interaction. By studying the interaction between a positively charged protein and negatively charged HS the emphasis is on electrostatic interactions. The properties of the complexes will be derived from the charging characteristics of the individual components and their complexes. The extent of mutual charge compensation in the HS–protein complex at its iso-electric point (IEP) will be investigated in detail. Some attention will be paid to the flocculation/precipitation of the complexes at the IEP and to the effect of the order of addition on the properties of the complexes. In the conclusion section the translation of the results to natural systems will be briefly discussed.

## 2. EXPERIMENTAL

### 2.1. Materials

#### 2.1.1. Purified Aldrich humic acid (PAHA)

Aldrich humic acid (Aldrich H1, 675-2) is purified using the method described by Vermeer et al. (1998). The final treatment with Dowex 50W-X8 was not carried out; after the other purification steps the level of trace metal ions is so low that it may be expected it will not significantly affect the protein binding. The obtained humic acid is freeze-dried and stored in a closed container that is placed in a desiccator with drying agent. The product is denoted as purified Aldrich humic acid (PAHA). According to Vermeer et al. (1998) the molar mass of PAHA as determined by viscometry and size exclusion chromatography is around 20 kDa and the elemental analysis on an ash free basis is: C, 55.8%; O, 38.9%; H, 4.6%; N, 0.6% (wt). A stock solution of 2 g PAHA/L is made in a volumetric flask by dissolving PAHA under mild shaking for about 24 h at pH 10. The high pH ensures that the PAHA is well dissolved (Avena and Wilkinson, 2002).

#### 2.1.2. Lysozyme (LSZ)

Hen egg-white lysozyme (L-6876; Molar mass 14.6 kDa) is purchased from Sigma and used without further purification. A space filling model of hen egg-white LSZ with colored functionalities has been presented by Horsley et al. (1987). The LSZ is dissolved in purified water to a concentration of 5 g/L. Other LSZ solutions are made from this stock solution. The LSZ stock solution is stored in the refrigerator at 5 °C to prevent degradation. LSZ in solution is stable in solutions ranging from moderately acidic to basic and even at the IEP which is around 10.5 no serious flocculation occurs.

#### 2.1.3. Water and chemicals

Water used for the experiments is twice de-ionized and filtered through an activated carbon column and a micro filter (EASY pure UV); it has a resistance greater than 18.3 MΩ/cm. The inorganic chemicals used are of analytical grade quality (obtained from Merck or Sigma–Aldrich). Titrant solutions of 0.1 mol/L HCl and KOH are obtained from Merck or Bernd Kraft and standardized before use.

### 2.2. Methods

#### 2.2.1. Potentiometric proton titrations

Proton titrations are performed using an automatic titration set-up consisting of a titration cell with a combined pH electrode (glass–Ag/AgCl), motor driven burettes and a Schott TR250 titration interface linked to the burettes and the electrodes. The cell is kept at $25.0 \pm 0.1$ °C using a water bath. Equipment and data acquisition are under PC control. In the titration cell 50 mL of sample (0.4 g PAHA/L, 1.0 g LSZ/L) or blank solution is added. After introduction of electrodes, burette tips, and the $N_2$ source, the cell is closed, the pH is adjusted to about 3 and a flux of nitrogen is passed through the solution to remove possible $CO_2$. After an equilibration time of at least 1 h the nitrogen

flux is maintained just above the solution and titrations are carried out from pH 3 to 11 and back. Standard solutions of 0.1 mol/L HCl and 0.1 mol/L KOH are used as titrants. $CO_2$ dissolution in the basic titrant is inhibited by a special lock containing an alkaline solution that prevents direct contact with air. Titrants (mostly 0.1 mol/L) are added in minimum aliquots of 0.01 ml HCl or KOH. After addition of titrant the rate of drift is measured over a 2 min interval. Electrode readings are accepted when the drift is less than 0.2 mV/min, but a maximum time of 20 min is set for two successive additions of titrant. After each cycle, the ionic strength is increased to the next higher level by adding KCl solution. After salt addition the cell is equilibrated for 20 min before continuation of the titration. For all KCl concentrations a blank titration (no PAHA or LSZ) is also performed. These blank titrations are fit to theoretical titration curves using the improved Davies equation (Davies, 1962) for the calculation of the mean ionic activity coefficient. When the mean activity coefficient is properly calculated, the Nernst plots of pH vs. the potential of the pH electrode with respect to the reference electrode (cell EMF in mV) derived from the blank titrations are independent of the salt concentration. The cell works properly when the latter is true and when the thus obtained Nernst plot is very similar to that obtained by simple calibration of the cell with buffer solutions.

Proton binding—pH curves of the samples are calculated by subtracting the calculated blank titration values from the measured titration points of the sample. By using the calculated blank the exact pH, volume and salt concentration as present during the sample titration can be used for the blank subtraction.

### 2.2.2. pH-stat titrations

The pH-stat titrations are also carried out with the Schott-titration set-up. To the titration cell 50 mL of 1 g/L LSZ or 0.4 g/L PAHA is transferred. The pH is brought to the desired value of 5 for PAHA and to 7 for LSZ by addition of 0.001 mol/L HCl or KOH. At the chosen pH values small releases of protons can be detected accurately. The sample is allowed to equilibrate to the chosen pH value for a couple of hours by adding small amounts of acid or base. Then some KCl solution is added and after an equilibration time of 20 min small additions of dilute acid or base solution are made to reach the pH-stat value. After each addition the cell is allowed to equilibrate. By taking a dilute titrant solution only acid or base can be used to reach the pH-stat value. The procedure is then repeated for the next KCl concentration. By subsequent KCl additions the concentration is stepwise increased to 5, 10, 20, 50, and 100 mmol/L KCl. From the added amount of titrant, the solution volume and the sample mass the change in proton binding of the sample can be calculated at each KCl concentration.

### 2.2.3. Particle charge detector/iso-electric-point measurements

Iso-electric-points (IEPs) of PAHA–LSZ complexes are measured using a "Mütek Particle Charge Detector" (PCD03-pH). The apparatus is also known as "streaming current meter". The sample cell is a cylindrical Teflon chamber in which a cylindrical Teflon piston moves up and down through the sample solution. The chamber is equipped with two gold electrodes connected to signal amplifier that presents a signal in mV. The signal is related to the streaming potential or streaming current of the particles present in the cell. Most common belief is that the colloidal particles stick to the walls of cell and piston and that the counterions move with the liquid (Dentel et al., 1989; Walker et al., 1996), but it is also possible that the colloidal particles and the mobile counterions in the solution move with different velocities (Müller, 1996). The method has been discussed in relation to other electrokinetic measurements by Barron et al. (1994). It is well-suited to measure the charge sign of the colloidal particles and, in the case of titrations with a complexing agent with a charge opposite to that of the particles, the point where the charge of the complex reverses its sign, i.e., the IEP of the complex.

With the PCD03 equipment a polyelectrolyte titrant solution is added with an automatic titrator (Mütek PCD-Two) in steps of 0.02 mL to the polyelectrolyte sample solution (25 mL) in the cell. The potentials (mV) are recorded together with the solution pH. From the titration curve the IEP is determined. The titration speed can be controlled within the range of 30–90 s per titrant addition. Both rates give the same IEP, which is the important parameter. The LSZ titrations with PAHA also give identical curves at 30 and 90 s/step, but the shape of the curves of the PAHA titration with LSZ differ somewhat at 30 and 90 s/step. In the presented results an addition rate of 30 s/step is used.

## 3. RESULTS

### 3.1. Proton binding to PAHA

With the pH-stat titration the amount of base that is required to maintain the PAHA suspension at pH 5 after each addition of KCl is measured. From the amount of base the release of protons $(-\Delta\Gamma_H)$ is calculated; at no added salt $\Delta\Gamma_H = 0$. The value of $-\Delta\Gamma_H$ (mmol/g) is depicted in Fig. 1 as a function of the KCl concentration. As expected, the proton dissociation is enhanced by increasing the KCl
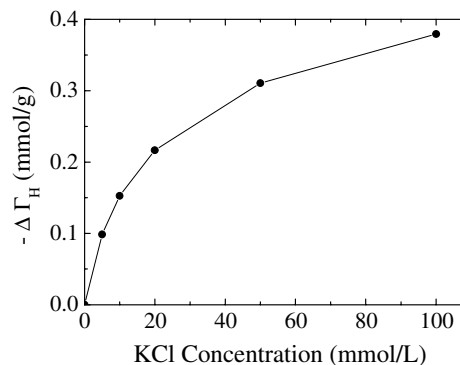


Fig. 1. Proton release, $-\Delta\Gamma_H$, by PAHA at pH 5 as a function of the KCl concentration.
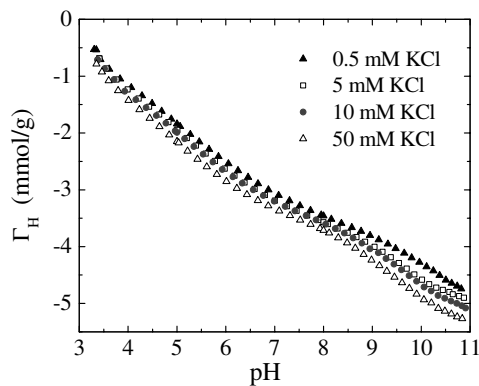
Fig. 2. Proton binding isotherms of PAHA at different KCl concentrations indicated in the figure (the concentration of KCl equals to the sum of the initial salt concentration in the HA solution and the concentration of KCl added).



Fig. 3. Proton uptake $\Delta\Gamma_H$ by LSZ at pH 7 as a function of the KCl concentration.



Fig. 4. Proton binding ($\Gamma_H$ in mmol/g) on LSZ as a function of pH at different KCl concentrations.

concentration. Below 20 mmol/L KCl the value of $-\Delta\Gamma_H$ increases relatively strongly, then it levels off.

The potentiometric titration curves are well reproducible and independent of the direction of the titration. From these titrations and the corresponding blank titrations the relative proton binding isotherms are obtained. According to Vermeer et al. (1998) the proton binding of PAHA at pH 5 and 10 mmol/L KCl is −1.95 mmol/g. This value is used as reference point. The absolute proton binding at other KCl concentrations and pH 5 can now be derived using the pH-stat results (Fig. 1). The resulting H-binding isotherms of PAHA at different KCl concentrations are shown in Fig. 2. The degree of dissociation of PAHA at a given pH increases with increasing salt concentration. The present data are in good agreement with those of Vermeer et al. (1998) for the same system (other batch and more stringent purification procedure) and in general agreement with the proton desorption behavior of other HA samples (Avena et al., 1999b; Milne et al., 2003).

### 3.2. Proton binding to LSZ

With the pH-stat titration the amount of acid required to maintain the LSZ suspension at pH 7 after addition of KCl is measured. The uptake of protons, $\Delta\Gamma_H$ (mmol/g), is depicted in Fig. 3 as a function of the KCl concentration; at no added salt $\Delta\Gamma_H$ is zero. The trend is similar to that observed for PAHA, but the magnitude of the effect is much smaller.

Also for LSZ the titration curves are reversible and well reproducible. The calculated proton binding ($\Gamma_H$) isotherms on LSZ at different KCl concentrations are shown in Fig. 4. According to Haynes et al. (1994) the net proton binding at pH 7 and 20 mmol/L KCl is 0.50 mmol/g (+7.34 net charges per protein molecule). This value is used as reference point. The absolute net proton binding at the present KCl concentrations and pH 7 are derived from this reference value and the pH-stat results (Fig. 3). The resulting reference points for the $\Gamma_H$-pH curves at 0.5, 5.0, 10, 50 mmol/L KCl and pH 7 are 0.49, 0.49, 0.50 and 0.51 mmol/g, respectively. From Fig. 4 it follows that the
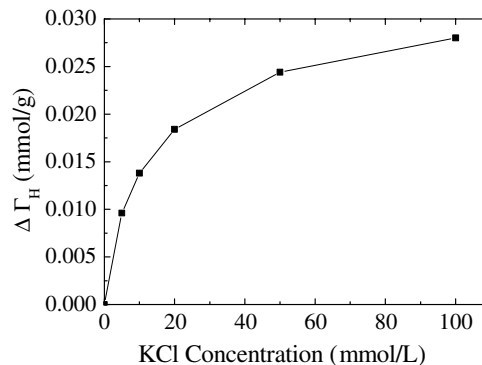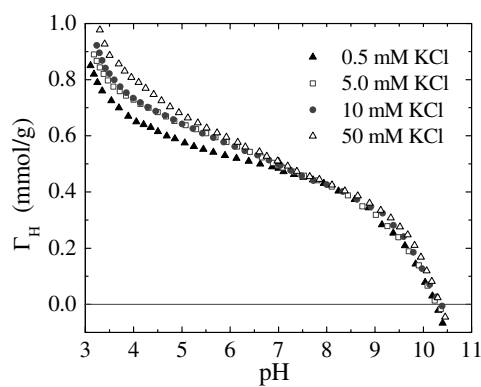
shift of the proton binding with increasing ionic strength is very limited, especially for pH >7. The point of zero charge (PZC) is found at pH 10.4, which is close to the theoretical PZC of 10.7 (Biesheuvel et al., 2005). The proton binding isotherms are similar to those reported in literature (Haynes et al., 1994; Biesheuvel et al., 2005), but more accurate with respect to the salt concentration effects. In the pH range from 4 to 7 the decrease in the net positive charge is largely due to increased dissociation of carboxyl groups in glutamic and aspartic acid residues, and at pH 7–10 to deprotonation of mainly the $\varepsilon$-amino groups in lysine and phenol groups in tyrosine.

### 3.3. PAHA interaction with LSZ

#### 3.3.1. Proton binding to PAHA–LSZ complexes

To investigate the proton binding to PAHA–LSZ complexes titrations are conducted of two mixtures of PAHA and LSZ in 5 mmol/L KCl. The mixtures are prepared by addition of PAHA to a LSZ solution, the total solution volume is 50 mL. The mass ratios, $f$, of PAHA to LSZ are 0.1 and 0.4. The proton binding isotherms of the mixtures are obtained by subtraction of the blank from the sample titration in the same way as described for the pure components. The experimental results are depicted in Fig. 5 by the solid symbols. Based on the Mütek experiments at 5 mmol/L
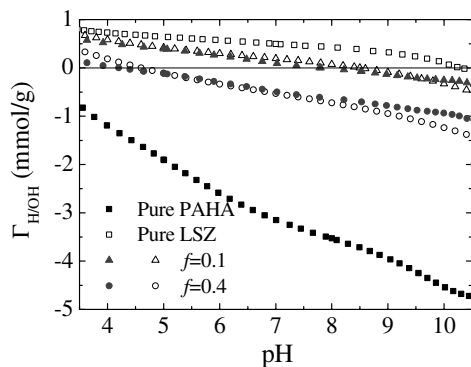
Fig. 5. Proton binding curves of pure LSZ and pure PAHA and two mixtures of PAHA and LSZ at 5 mmol/L KCl; $f$ equals the mass ratio of g PAHA to g LSZ. The solid symbols represent the experimental values. The experimental curves are fixed at their measured $pH_{IEP}$ values under the assumption that $pH_{PZC} = pH_{IEP}$. Open symbols represent the calculated proton binding obtained by assuming that PAHA and LSZ do not interact (mass weighted summation of PAHA and LSZ proton binding at 5 mmol/L KCl).

KCl, to be discussed in the next sections, $pH_{IEP}$ values at $f = 0.1$ and 0.4 can be obtained by linear extrapolation of the graph of $f_{IEP}$ vs. $pH_{IEP}$; they are 7.8 and 4.2, respectively. By assuming that at low KCl concentration $pH_{PZC} = pH_{IEP}$ these values have been used as reference points for the two experimental isotherms. At pH values around $pH_{IEP}$ of the complex it may be expected that all LSZ and PAHA is present as complex. Theoretical proton binding isotherms obtained by using a simple mass weighted additivity are also included in Fig. 5 (open symbols). The 'additivity rule' assumes that PAHA and LSZ do not change their proton binding upon interaction. The calculated $pH_{PZC}$ values are, respectively, 8.5 at $f = 0.1$ and 4.6 at $f = 0.4$. These values are somewhat higher than the corresponding $pH_{IEP}$ values, but it should be realized that only a small shift (0.1 mmol/g) in proton binding leads to a good match.

In general, the experimental curves differ only little from the theoretical ones in the pH range 4.5–8.0. This implies that the interaction of PAHA and LSZ in the complex does not lead to a large uptake or exclusion of protons. Both at low and high pH the measured proton binding changes slightly less than the theoretical one. At low pH this can be explained by a somewhat better dissociation of acidic groups of PAHA in the complex because the screening of the negative PAHA charges by positive LSZ is slightly better than that by 5 mmol/L KCl. At high pH PAHA is highly negative and the interaction slightly increases the positive charge of LSZ in the complex. Overall, the conclusion is that the charge adaptation due to interaction is small.

### 3.3.2. Electrokinetic charge neutralization in PAHA–LSZ complexes at their IEP

#### 3.3.2.1. LSZ titration by PAHA at pH 5.
The Mütek titration curves of LSZ by PAHA for three different amounts of LSZ, initial pH of 5 and 5 mmol/L KCl are depicted in Fig. 6. Together with the Mütek potential the pH change is also plotted. At pH 5 LSZ has a net positive charge, so
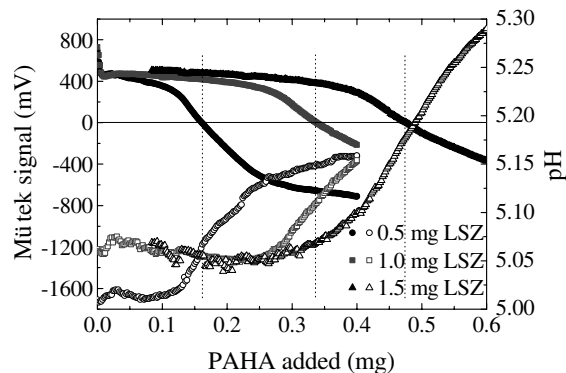


Fig. 6. Titration curves of LSZ by PAHA in 5 mmol/L KCl solution and initial pH of 5. The solid symbols present the potential (mV) and open symbols the pH.

the Mütek potential (mV) starts positive. The signal decreases sharply with the first additions of PAHA, then the decrease becomes very weak until close to the IEP. Around the IEP, where the signal reflects the behavior of the PAHA–LSZ complexes, the potential decreases strongly and at the IEP the signal changes from positive to negative; this implies that beyond the IEP a super-equivalent amount of negative PAHA is bound to positive LSZ.

The pH value is somewhat unstable in the first part of the titration and increases most strongly around the IEP. The increase in pH reflects a proton uptake by the complex as a result of the interaction. Less protons in solution corresponds with an increase of the number of positively charged groups of LSZ in the complex. The net adjustment in proton binding at the IEP is about 0.03 mmol/g complex. This is only 5% of the net proton binding to 1 g LSZ at pH 5 and 5 mmol/L KCl. The pH values at the IEP of the PAHA–LSZ complexes are about 5.1.

Similar titrations are carried out for two other KCl concentrations and initial pH 5. Fig. 7 depicts for the three KCL concentrations the amounts of PAHA needed to reach the IEPs of PAHA–LSZ complexes when different amounts of LSZ are present in the cell. In all three cases
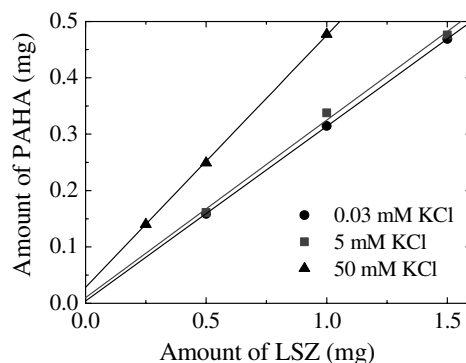


Fig. 7. Amount of PAHA to reach the IEP of the LSZ–PAHA complex (PAHA is titrant) at the initial pH of 5 and various added KCl concentrations. The average pH values at the IEP and 0.03, 5 and 50 mmol/L KCl are 5.1, 5.1, and 5.2, respectively.

the dependence is linear. The line for no added KCl (ionic strength about 0.03 mmol/L) passes within experimental error through the origin, the lines for 5 and 50 mmol/L KCl intersect the *Y*-axis at 0.01 and 0.03 mg PAHA. These values corresponds to, respectively, 0, 0.4 and 1.2 mg/L PAHA at the IEP of the complex. Therefore, the PAHA binding to LSZ has a high affinity, but the affinity weakens slightly with increasing KCl concentration. The slopes of the lines equal the PAHA/LSZ mass ratios in the complex at the IEP. The mass ratios are 0.31, 0.32 and 0.45 at, respectively, 0.03, 5, and 50 mmol/L KCl; i.e., at 50 mmol/L about 45% more PAHA is required to reach the IEP than at low ionic strength. In other words, at high ionic strength there is less LSZ needed to neutralize the negative charge of PAHA. Assuming that at 0.03 mmol/L KCl the charge compensation of PAHA is completely due to LSZ and comparing the mass ratios at 0.03 and 50 mmol/L KCl reveals that at 50 mmol/L KCl around 40% of the negative PAHA charge in the complex is compensated by $K^+$ instead of by the positive LSZ charge.

The behavior can be further characterized by comparing the charges of PAHA and LSZ obtained from the potentiometric titrations. The PAHA/LSZ charge ratio varies between 3.11 and 2.97 depending on the KCl concentration. Therefore with a 1:1 stoichiometry a PAHA/LSZ mass ratio of 0.32–0.34 would be required for charge neutralization. These values are in close agreement with the mass ratios at the IEP for no added KCl and 5 mmol/L KCl. This indicates that the LSZ charge is indeed fully compensated by the PAHA charge and that most likely there is no or very little net charge adjustment upon complexation. At 50 mmol/L KCl the mass ratio of 0.34 for charge neutralization is much smaller than the mass ratio at the IEP (0.45). Comparison of these ratios indicates that 32% of the PAHA charge in the complex is compensated by $K^+$. This value is more accurate than the estimate based on the Mütek results only, because with the Mütek results two different salt concentrations are compared and the salt concentration as such is affecting the charge of both PAHA and LSZ (see Figs. 2 and 4).

*3.3.2.2. LSZ titration by PAHA at pH 8.* To change the charge ratio Mütek titrations of LSZ with PAHA are also carried out at an initial pH 8. Compared to pH 5 the negative charge of PAHA is considerably higher and the positive charge of LSZ is a bit lower. The titration results are depicted in Fig. 8. Initially the Mütek potential is behaving differently from the previous titration: after a slight decrease a substantial increase in positive signal is observed. Close to the IEP the behavior is similar: a decreasing potential that changes sign at the IEP (the region beyond the IEP was not followed). The behavior of the pH is also different: first a weak maximum followed by a relatively large decrease and an almost constant pH around the IEP. The proton release corresponds with the increase of the Mütek potential. Possibly PAHA releases only a few protons (about 0.05 μmol) upon complexation with LSZ, but due to the close to neutral initial pH of the solution, the small amount of protons released has led to a significant pH decrease: the initial pH 8 reduces to a final pH of about 7. The
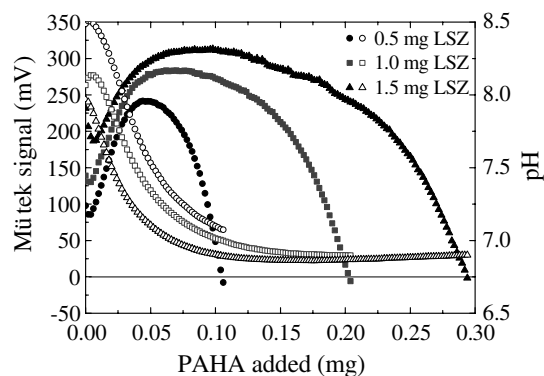


Fig. 8. Titration curves of LSZ by PAHA in 5 mmol/L KCl solution and initial pH of 8. The solid symbols present the potential (mV) and open symbols the pH. The pH of the IEPs is around 7.

pH change in solution leads to an increase of the charge of the free LSZ and this is noticed with the increase of the Mütek signal. When the Mütek signal decreases strongly all LSZ has formed complexes with PAHA and the pH of about 7 hardly changes, therefore no significant adjustment of net proton binding occurs.

Further titrations are carried out at other KCl concentrations. The amounts of PAHA needed to reach the IEP of the LSZ–PAHA complexes (final pH about 7) are depicted in Fig 9. Again straight lines are observed; with no added KCl the line passes through the origin, and for 5 and 50 mmol/L KCl the lines intersect with the *Y*-axis at 0.01 and 0.02 mg PAHA. These intercepts correspond to solution concentrations of 0, 0.4 and 0.8 mg/L, respectively. Therefore, also in this case the affinity between LSZ and PAHA at the IEP is high and very similar to that at pH 5. The PAHA/LSZ mass ratios at the IEP (slopes) are 0.17, 0.19 and 0.25 in, respectively, 0.02, 5, and 50 mmol/L KCl. These ratios are lower than those at pH 5 due to a less positive charge of LSZ and a more negative charge on PAHA. Comparing the mass ratio at no added salt with those at 5 and 50 mmol/L KCl indicates that 12% and 47%, respectively, of the PAHA charge is compensated by $K^+$ at these two KCl concentrations.
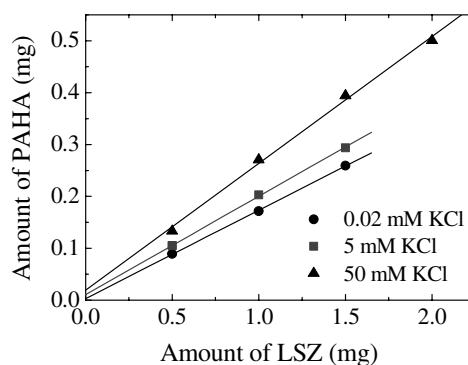


Fig. 9. The amount of PAHA needed to reach the IEP of the LSZ–PAHA complex (PAHA titrant) at a final pH of about 7 (initial pH 8) and three KCl concentrations.

As before, these mass ratios may be compared with the mass ratios derived from the potentiometric titration charges at pH 7 (the pH at the IEP) and assuming a 1:1 stoichiometry. The latter ratios range from 0.17 to 0.16 for the different KCl concentrations. At no added KCl the mass ratio at the IEP is in close agreement with the mass ratio derived from potentiometry; the PAHA charge neutralizes the LSZ charge and there is no net charge adjustment. A similar comparison at 5 and 50 mmol/L KCl indicates that, respectively, 14% and 56% of the PAHA charge in the complex is compensated by $K^+$. These values are similar to those obtained by using the Mütek results only.

*3.3.2.3. PAHA titration by LSZ at pH 5.* Instead of adding PAHA to LSZ during the titration, one can also add LSZ to a solution containing PAHA. Fig. 10 depicts the titration curves of PAHA by LSZ for three different amounts of PAHA at an initial pH of 5 and 5 mmol/L KCl. Initially the potential increases slowly with the addition of LSZ, then it increases sharply and somewhat before the IEP is reached the curves level off again. Although the slope around the IEP is gradual, it is not difficult to obtain the IEP. The pH increases most strongly in the initial part of the titration and around the IEP the pH hardly changes. The pH of the IEP is about 5.2. The relatively small changes of the potential around the IEP are different from the observations for the reversed titration. This indicates that the complex formation and probably the complex structure at the IEP depend on the sequence of addition. From the increase in pH up to the IEP a proton uptake by the complex ranging from 0.006 to 0.015 mmol/g complex is found. This is somewhat less than with the reverse titration sequence and very small compared to the proton binding to 1 g PAHA or 1 g LSZ at pH 5 and 5 mmol/L KCl.

In addition to the results shown in Fig. 10 two further titrations were made at 0.05 and 0.30 mg PAHA. The amounts of LSZ needed to reach the IEP of PAHA–LSZ complex at pH 5 and 5 mmol/L KCl are summarized in Fig. 11 (squares). For easy comparison the results for PAHA addition to LSZ are also shown (triangles). As before a straight line is observed that has a small intercept. Clearly the high affinity character of the binding at the
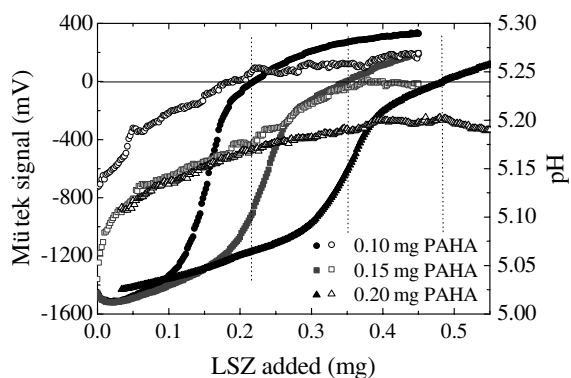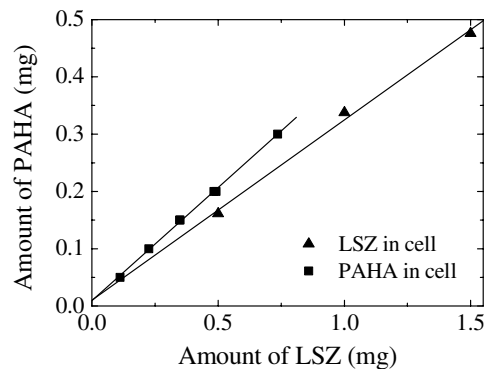


Fig. 11. PAHA–LSZ complexation at about pH 5 and 5 mmol/L KCl. Triangles: PAHA addition to LSZ; squares: LSZ addition to PAHA.

IEP is not affected by the order of addition. The PAHA/LSZ mass ratios (slopes) at the IEP are for LSZ addition to PAHA 0.40 and for PAHA addition to LSZ 0.31. The latter value corresponds closely with the mass ratio derived from the potentiometric titration results. However, upon addition of LSZ to PAHA 27% more PAHA is required to reach the IEP than when PAHA is added to LSZ. Even at 5 mmol/L KCl, the complex that is formed when LSZ is added to PAHA is far removed from the 1:1 stoichiometry. This implies a complex at the IEP in which a substantial amount of $K^+$ is incorporated at only 5 mmol/L KCl. This, in turn, is a strong indication that PAHA in the complex is also internally aggregated, 27% of the negative groups of PAHA are not in direct contact with the positive groups of LSZ. The fact that the complexes at their IEP are dependent on the order of addition also indicates that the equilibrium structure is not reached. Most likely the complex formed by addition of LSZ to PAHA, which includes considerable amounts of $K^+$, is trapped in a local Gibbs energy minimum.

*3.3.3. Flocculation of PAHA–LSZ complexes at the IEP*

Preliminary experiments show that at pH 5 and 5 mmol/L KCl the order of additions is also of relevance for the flocculation and precipitation of PAHA–LSZ complexes at the IEP. During the titration of 0.20 mg PAHA by LSZ no precipitate is observed in the Mütek cell. However, by keeping the complex at rest at the IEP a precipitate appears after 6 h. Photographs of the sample at different waiting times are shown in Fig. 12. For the titration of 1.5 mg LSZ by PAHA, under the same conditions, a similar test was conducted but here no precipitate is observed after keeping the complex at the IEP for 12 h. Therefore, the spatial structure and internal stability of the complexes in the IEP also depend on the order of addition. In general, the stability behavior of the PAHA–LSZ complexes is in contrast with the stability of HA complexes with strong cationic flexible polyelectrolytes. The latter class of polyelectrolytes is used for effective removal of HA form solution by bringing the complex to its IEP. At the IEP the complexation is succeeded by quick aggregation and precipitation (Bolto et al., 1999; Kam and Gregory, 1999; Kam and Gregory, 2001).



Fig. 10. Titration curves of PAHA by LSZ in 5 mmol/L KCl and pH about 5. Solid symbols present the Mütek signal (mV) and open symbols the pH.
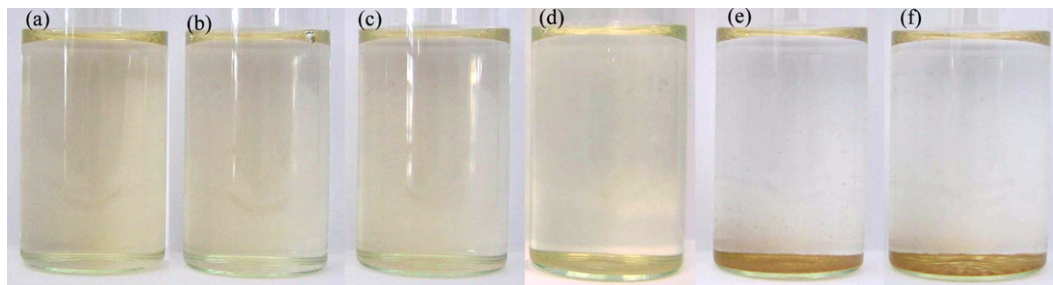
Fig. 12. Photographs of the dispersion of the PAHA–LSZ complex at the IEP after different waiting times (pH 5 and 5 mmol/L KCl). The dispersion of the complex is made by slowly adding LSZ to PAHA till the IEP is reached. (a) Original solution of 8 mg PAHA/L after 24 h; (b) complex after reaching the IEP (0 h); complex at the IEP after 2 h at rest (c), 6 h (d), 12 h (e) and 24 h (f).

## 4. CONCLUSIONS AND DISCUSSION

PAHA and LSZ form complexes in the pH range where the PAHA charge is negative and the LSZ charge positive. Both at pH 5 and pH 7 the affinity between PAHA and LSZ is high. Yet, there is little net charge adaptation upon forming the complex. This might indicate that the charged groups of HA and LSZ in the complex are in "loose contact", which is probably due to the fact that both LSZ and PAHA are internally structured polyelectrolytes. Complexes that are formed just before their IEP is reached will still be present beyond the IEP, but by passing the IEP the charge sign of the complex changes. This implies that in the presence of an excess of HA the PAHA–LSZ complexes are negatively charged and with an excess of LSZ positively charged.

At pH 5 and low KCl concentrations (5 mmol/L) the PAHA–LSZ complexes formed by adding PAHA to LSZ contain little or no $K^+$ at the IEP of the complex, however, when LSZ is added to PAHA 27% of the PAHA charge is balanced by $K^+$. The fact that the structure of the complexes at the IEP depends on the order of addition is also reflected in the stability. PAHA–LSZ complexes at the IEP that are formed by adding PAHA to LSZ show no precipitation after standing 12 h, whereas complexes formed by addition of LSZ to PAHA slowly precipitate.

At higher KCl concentration the PAHA–LSZ complexes formed by PAHA addition to LSZ also contain $K^+$; at 50 mmol/L and pH 5 about 30–40% of the PAHA charge in the complex is balanced by $K^+$ and at pH 7 about 45–55%.

Incorporation of $K^+$ in the PAHA–LSZ complexes at the IEP strongly suggests that the PAHA molecules in these complexes are partly aggregated. Qualitatively this corresponds with the view that HA molecules/building blocks in solution form weak aggregates/micelles (Avena and Wilkinson, 2002; Sutton and Sposito, 2005). For PAHA the presence of such aggregates can be derived from the dynamic light scattering (DLS) measurements of Vermeer (Vermeer, 1996: Vermeer et al., 1998). These measurements reveal particles with radii ranging from about 65 to 75 nm depending on pH (4.5–8.5) and $KNO_3$ concentration (1–100 mmol/L). The large values point to PAHA aggregates. Single PAHA molecules are most likely only a few nanometers and too small to be detected by DLS. According to

Avena and Wilkinson (2002) HA aggregates are in dynamic equilibrium with the HA monomers. Their results at 5 mmol/L 1-1 electrolyte and peat HA show that at high pH the disaggregation rate is extremely rapid, at intermediate pH disaggregation occurs within an hour and at low pH the disaggregation takes a month. Clearly such HA aggregation behavior can also strongly affect the complex formation of PAHA and LSZ at pH 5 and 7. For instance, adding at low salt concentration PAHA to an abundance of LSZ probably leads to HA-disaggregation, therefore the PAHA–LSZ complex hardly contains $K^+$. Adding LSZ to a solution with PAHA more likely gives fragments of aggregated PAHA that are complexed with LSZ and such complexes will also contain $K^+$. At higher electrolyte concentrations disaggregation of the PAHA aggregates is slower and here $K^+$ incorporation even occurs when PAHA is added to LSZ. Further aggregation of primary PAHA–LSZ complexes to large flocs that can settle is an important step for the precipitation of these complexes at their IEP. This step will also be affected by the primary structure of the complex. By increasing the salt concentration more $K^+$ will be incorporated in the primary complexes and large floc formation will be counteracted by disaggregation of the partial PAHA aggregates in the flocs. On the other hand large floc formation will be promoted by increasing the salt concentration, because the electrostatic repulsion between the primary PAHA–LSZ complexes decreases.

The above conclusions are most likely also relevant for other HA–protein systems, as long as the protein is positively charged and internally well structured. In general, it may be clear that for a good understanding of HA–protein complexation more study is required. The present study indicates that HA–protein interaction easily occurs when the protein is positively charged. The affinity for complexation is high and this implies that already at concentrations in the 1–10 mg/L range complexes are formed. The structure and fate of the primary complexes depends on conditions such as pH (charge of the particles), salt concentration, relative abundance of protein compared to HA, sequence of addition and type of protein. The fact that the HA–protein complexes do not quickly precipitate implies that such complexes may have the time to adsorb to mineral surfaces. This could be of special relevance in the case of a positive complex and silica which is mostly negatively charged. Normally HA does not bind to silica, but

HA complexed with a cationic protein can bind and this will affect the characteristics of the silica particles and may even affect soil structure. Preliminary experiments of sequential addition of LSZ and PAHA to silica indeed reveal that LSZ–PAHA multilayer formation occurs on the silica surface.

The present study does not give information on activity of the protein in the PAHA–LSZ complexes. To be able to answer this question more information is required on the structure of the complexes, the reversibility of the complexes and on structural rearrangements in the protein molecule upon binding to HA. Alteration in protein structure and, hence, in bioactivity is a common phenomenon when a protein enters another environment (Zoungrana et al., 1997). In particular the interaction with hydrophobic species induces changes in the protein structure (Haynes and Norde, 1994). From cationic surfactant binding studies to humic and fulvic acids it is found that hydrophobicity of HA is important for the interaction (Ishiguro et al., 2007). Therefore hydrophobic interaction will most likely also play a role with HA–protein complexation. In a future paper we will study complex and aggregate formation in more detail (using DLS) by following the course of complexation and aggregation during titration of HA with protein and the reverse. Preliminary results indicate that the formation of the complexes is partly reversible. This implies that the protein could still interact with other substances. Therefore, competitive binding involving other substances may affect the protein activity.

## REFERENCES

Adou A. F. Y., Muhandiki V. S., Shimizu Y. and Matsui S. (2001) A new economical method to remove humic substances in water: adsorption onto a recycled polymeric material with surfactant addition. *Water Sci. Technol.* **43**, 1–7.

Avena M. J., Vermeer A. P. W. and Koopal L. K. (1999a) Volume and structure of humic acids studied by viscometry: pH and electrolyte concentration effects. *Colloids Surfaces A* **151**(1999), 213–224.

Avena M. J., Koopal L. K. and van Riemsdijk W. H. (1999b) Proton binding to humic acids: electrostatic and intrinsic interactions. *J. Colloid Interface Sci.* **217**, 37–48.

Avena M. J. and Wilkinson K. J. (2002) Disaggregation kinetics of a peat humic acid: mechanism and pH effects. *Environ. Sci. Technol.* **36**, 5100–5105.

Barron W., Murray B. S., Scales P. J., Healy T. W., Dixon D. R. and Pascoe M. (1994) The streaming current detector: a comparison with conventional electrokinetic techniques. *Colloids Surfaces A* **88**, 129–139.

Blake C. C. F., Koenig D. F., Mair G. A., North A. C. T., Phillips D. C. and Sarma V. R. (1965) Structure of hen egg-white lysozyme—a 3-dimensional fourier synthesis at 2a resolution. *Nature* **206**, 757–761.

Biesheuvel P. M., van der Veen M. and Norde W. (2005) A modified Poisson–Boltzmann model including charge regulation for the adsorption of ionizable polyelectrolytes to charged interfaces, applied to lysozyme adsorption on silica. *J. Phys. Chem. B.* **109**, 4172–4180.

Bohidar H., Dubin P. L., Majhi P. R., Tribet C. and Jaeger W. (2005) Effects of protein–polyelectrolyte affinity and polyelectrolyte molecular weight on dynamic properties of bovine serum albumin—poly (diallyldimethylammonium chloride) coacervates. *Biomacromolecules* **6**, 1573–1585.

Bolto B. A. (1995) Soluble polymers in water purification. *Prog. Polym. Sci.* **20**, 987–1041.

Bolto B., Abbt-Braun G., Dixon D., Eldridge R., Frimmel F., Hesse S., King S. and Toifl M. (1999) Experimental evaluation of cationic polyelectrolytes for removing natural organic matter from water. *Water Sci. Technol.* **40**, 71–79.

Buffle J. (1988) *Complexation Reactions in Aquatic Systems*. Ellis Horwood Ltd., Chichester.

Brouwer M., Cashon R. and Bonaventura J. (1990) Functional-properties of hemoglobin immobilized in coacervates prepared from gelatin-a and polyanionic carbohydrates. *Biotechnol. Bioeng.* **35**, 831–836.

Carlsson F., Linse P. and Malmsten M. (2001) Monte Carlo simulations of polyelectrolyte–protein complexation. *J. Phys. Chem. B* **105**, 9040–9049.

Coffman J. L., Lightfoot E. N. and Root T. W. (1997) Protein diffusion in porous chromatographic media studied by proton and fluorine PFG-NMR. *J. Phys. Chem. B* **101**, 2218–2223.

Cooper C. L., Dubin P. L., Kayitmazer A. B. and Turksen S. (2005) Polyelectrolyte–protein complexes. *Curr. Opin. Colloid Interface Sci.* **10**, 52–78.

Davies C. W. (1962) *Ion Interactions*. Butterworth, London, p. 43.

Dentel S. K., Thomas A. V. and Kingery K. M. (1989) Evaluation of the streaming current detector: 1 Use in jar tests. *Water Res.* **23**, 413–421.

Doublier J. L., Garnier C., Renard D. and Sanchez C. (2002) Protein–polysaccharide interactions. *Curr. Opin. Colloid Interface Sci.* **5**, 202–214.

Duval J. F. L., Wilkinson K. J., van Leeuwen H. L. and Buffle J. (2005) Humic substances are soft and permeable: evidence from their electrophoretic mobilities. *Environ. Sci. Technol.* **39**, 6435–6445.

Glaser H. T. and Edzwald J. K. (1979) Coagulation and direct filtration of humic substances with polyethylenimine. *Environ. Sci. Technol.* **13**, 299–305.

Gummel J., Boue F., Deme B. and Cousin F. (2006) Charge stoichiometry inside polyelectrolyte–protein complexes: a direct SANS measurement for the PSSNa-lysozyme system. *J. Phys. Chem. B* **110**, 24837–24846.

Hankins N. P., Lu N. and Hilal N. (2006) Enhanced removal of heavy metal ions bound to humic acid by polyelectrolyte flocculation. *Sep. Purif. Technol.* **51**, 48–56.

Hayes M. H. B. and Edward Clapp C. E. (2001) Humic substances: considerations of compositions, aspects of structure and environmental influences. *Soil Sci.* **166**, 723–737.

Haynes C. A., Sliwinsky E. and Norde W. (1994) Structural and electrostatic properties of globular-proteins at a polystyrene water interface. *J. Colloid Interface Sci.* **164**, 394–409.

Haynes C. A. and Norde W. (1994) Globular proteins at solid–liquid interfaces. *Colloids Surfaces B: Biointerfaces* **2**, 517–566.

Horsley D., Herron J., Hlady V. and Andrade J. D. (1987) Human and hen lysozyme adsorption: a comparative study using total internal reflection fluorescence spectroscopy and molecular graphics. In *Proteins at Interfaces* (eds. J. L. Brash and T. A.

Horbett). ACS Symposium Series343, Washington DC, U.S.A. pp. 290–305.

Ishiguro M., Tan W. F. and Koopal L. K. (2007) Binding of cationic surfactants to humic substances. *Colloids Surfaces A* **306**, 29–39.

Kam S. K. and Gregory J. (1999) Charge determination of synthetic cationic polyelectrolytes by colloid titration. *Colloids Surfaces A* **159**, 165–179.

Kam S. K. and Gregory J. (2001) The interaction of humic substances with cationic polyelectrolytes. *Water Res.* **35**, 3557–3566.

Koopal L. K., Goloub T. P. and Davis T. A. (2004) Binding of ionic surfactants to purified humic acid. *J. Colloid Interface Sci.* **275**, 360–367.

Koopal L. K., Saito T., Pinheiro J. P. and van Riemsdijk W. H. (2005) Ion binding to natural organic matter: general considerations and the NICA-Donnan model. *Colloids Surfaces A* **265**, 40–54.

Kokufuta E. (1994) Complexation of proteins with polyelectrolytes in a salt-free system and biochemical characteristics of the resulting complexes. In *Macromolecular Complexes in Chemistry and Biology* (eds. Dubin, Bock, Davis, Schulz and Thies). Springer-Verlag, Berlin, pp. 301–325.

Kvinnesland T. and Ødegaard H. (2004) The effects of polymer characteristics on nano particle separation in humic substances removal by cationic polymer coagulation. *Water Sci. Technol.* **50**, 185–191.

Merdy P., Huclier S. and Koopal L. K. (2006) Modeling metal–particle interactions with an emphasis on natural organic matter. *Environ. Sci. Technol.* **40**, 7459–7466.

Milne C. J., Kinniburgh D. G., van Riemsdijk W. H. and Tipping E. (2003) Generic NICA-Donnan model parameters for metal–ion binding by humic substances. *Environ. Sci. Technol.* **37**, 958–971.

Müller H. M. (1996) Zetapotential in der laborpraxis. Wissenschaftliche Verlagsgesellschaft, GmbH, Sturtgart, Germany.

Nichols K. A. and Wright S. F. (2005) Comparison of glomalin and humic acid in eight native U.S. soils. *Soil Sci.* **170**, 985–997.

Ramanadham M., Sieker L. C. and Jensen L. H. (1990) Refinement of triclinic Lysozyme. 2. The method of stereochemically restrained least-squares. *Acta Crystallogr. B* **46**, 63–69.

Rebhun M., Meir S. and Laor Y. (1998) Using dissolved humic acid to remove hydrophobic contaminants from water by complexation-flocculation process. *Environ. Sci. Technol.* **32**, 981–986.

Schindler F. V., Mercer E. J. and Rice J. A. (2007) Chemical characteristics of glomalin-related soil protein (GRSP) extracted from soils of varying organic matter content. *Soil Biol. Biochem.* **39**, 320–329.

Schmitt C., Sanchez C., Desobry-Banon S. and Hardy J. (1998) Structure and technofunctional properties of protein–polysaccharide complexes: a review. *Crit. Rev. Food Sci. Nutr.* **38**, 689–753.

Sutton and Sposito (2005) Molecular structure in soil humic substances: the new view. *Environ. Sci. Techol.* **39**, 9009–9015.

Tipping E. (2002) *Cation binding by humic substances.* Cambridge University Press.

Traina S. J., McAvoy D. C. and Versteeg D. J. (1996) Association of linear alkylbenzenesulfonates with dissolved humic substances and its effect on bioavailability. *Environ. Sci. Technol.* **30**, 1300–1309.

Tribet C. (1999) Complexation between amphiphilic polyelectrolytes and proteins: from necklaces to gels in Physical chemistry of polyelectrolytes (eds. T. Radeva). *Surfactant Science Series*, 99, M. Dekker, New York, pp. 687–741.

Vermeer A. W. P., van Riemsdijk W. H. and Koopal L. K. (1998) Adsorption of humic acid to mineral particles: 1. Specific and electrostatic interactions. *Langmuir* **14**, 2810–2819.

Vermeer A. W. P. (1996) Interactions between humic acid and hematite and their effects on metal ion speciation. Ph.D. thesis, Wageningen University, p. 63.

Walker C. A., Kirby J. T. and Dentel S. K. (1996) The streaming current detector: a quantitative model. *J. Colloid Interface Sci.* **182**, 71–81.

Wen Y. P. and Dubin P. L. (1997) Potentiometric studies of the interaction of bovine serum albumin and poly(dimethyldiallyammonium chloride). *Macromolecules* **30**, 7856–7861.

Xia J. and Dubin P. L. (1994) Protein–polyelectrolyte complexes. In *Macromolecular Complexes in Chemistry and Biology* (eds. Dubin, Bock, Davis, Schulz and Thies). Springer-Verlag, Berlin, pp. 247–271.

Xia J., Mattison K. W., Romano V., Dubin P. L. and Muhoberac B. B. (1997) Complexation of trypsin and alcohol dehydrogenase with poly(diallyldimethylammonium chloride). *Biopolymers* **41**, 359–365.

Zoungrana T., Findenegg G. H. and Norde W. (1997) Structure, stability and activity of adsorbed enzymes. *J. Colloid Interface Sci.* **190**, 437–448.

*Associate editor:* Michael L. Machesky